GEOCHRONOMETRIA Vol. 25, pp 19-28, 2006 – *Journal on Methods and Applications of Absolute Chronology*

THE LINEARLY MODULATED IRSL RED EMISSION FROM FELDSPARS

M. FATTAHI [1,2], J. S. SINGARAYER [3], R. M. BAILEY [4] and S. STOKES [2]

[1] Institute of Geophysics, University of Tehran, P.O. Box 14155-6466, Tehran, Iran
[2] School of Geography, Oxford University centre of Environment, South Parks Road Oxford OX1 3Q Y , U.K.
(e-mail: morteza.fattahi@ouce.ox.ac.uk)
[3] School of Geographical Sciences, Bristol University, University Road, Bristol, BS8 1SS, U.K.
[4]Department of Geography, Royal Holloway, University of London, Egham, Surrey, TW20 OEX, UK.

Key words: LUMINESCENCE DATING, FELDSPAR, RED EMISSION, LINEAR MODULATION

Abstract: **This paper uses the linear modulation technique to study red IRSL emission of potassium feldspars. Sub-samples were subjected to various pre-treatment and measurement conditions in an attempt to understand the relevant mechanisms of charge transfer. The linear modulation curves fitted most successfully to a sum of three first order components and we present supporting empirical evidence for the presence of three separate signal components. Additionally, the form of the red emission was observed to closely resemble the UV emission, implying the same donor charge concentrations may supply different recombination centres (assuming emission wavelength depends on centre type).**

1. INTRODUCTION

Feldspars in dosimetry

Felspathic minerals are one of the most abundant mineral groups found in sedimentary deposits and are also the most abundant mineral constituents of igneous rocks. There are several intrinsic advantages to using feldspars for dating geological and archaeological deposits over other minerals, such as the potential for dating over a wide time range, the relatively high luminescence sensitivity to dose, ease of light collection (due to stimulation/emission bands), and the considerable internal dose of K-feldspars which in many cases reduces the uncertainty in estimation of the total dose rate (Duller, 1997; Fattahi and Stokes, 2003a).

Methodologies using thermoluminescence (TL) and optically stimulated luminescence (OSL) of feldspars for dating of sedimentary deposits were pioneered by Mejdahl (e.g. 1985). However, the routine use of feldspars for dating has been blighted by significant age underestimations in many applications (e.g. Spooner and Questiaux, 1989). This effect has been especially pronounced in sediments older than 100ka. The phenomenon referred to as *anomalous fading* (where observed signal stability is lower than that predicted from kinetic analyses) has been observed for feldspars, with varying degrees of severity, by several authors (e.g. Wintle, 1973; Visocekas, 1985). It has been generally assumed that it is this signal instability that has led to the majority of observed underestimations (Visocekas, 1985).

Several approaches have been proposed to overcome the effect of anomalous fading (e.g. Lamothe and Auclair, 2000), most of which involve extrapolation of measured laboratory fading rates to correct for anomalous fading. An alternative approach is to look for a non-fading signal. Several authors (e.g. Zink, 1996; Fattahi, 2001), have noted that many feldspars exhibit a far-red TL emission band (590-750nm), as well as the commonly used UV/blue emission (~400nm). In a further detailed study, Zink and Visocekas (1997) observed that, while anomalous fading in many cases reduced the UV/blue emission, the far-red emission of samples of sanidine appeared unaffected. This led Visocekas (2000) to a new approach of monitoring anomalous fading of feldspar TL using ratios of the blue to far-red TL emissions. Importantly, Zink and Visocekas (1997) successfully dated three feldspars of volcanic origin using the far-red TL emission alone with an additive-dose protocol.

While, there is much potential in the far-red TL feldspar signal for dating, a considerable drawback to studies of the emission (590 - 750nm) is the significant blackbody component at the high temperatures necessary for TL measurement. This limited many previous TL measurements to temperatures below 350°C (Zink and Visocekas, 1997). Fattahi and Stokes (2000a) outlined an arrangement to detect the red emission band (590-700nm), allowing TL detection up to 600°C. Optical bleaching of far-red TL using several stimulating wavelengths was studied previously (e.g. Zink and Visocekas, 1997; Fattahi and Stokes, 2003b), however, Fattahi (2001) was the first to use infrared photons to optically stimulate far-red luminescence (hereafter this emission is termed IRSL (>600nm)), made possible by the new experimental set up.

As most feldspars exhibit this far-red emission band (Zink and Visocekas, 1997), which from previous studies, appears not to fade appreciably (Fattahi, 2001; Fattahi and Stokes, 2003b; 2004) it is worthy of extensive study, particularly since it's upper age limit is likely to reach well beyond that of quartz (currently the most commonly used mineral for luminescence dating of geological and archaeological deposits), possibly even exceeding 1Ma (Fattahi and Stokes, 2000b). As part of this research, it is necessary to study key aspects of the luminescence signal that relate to dating, and this paper forms a small component of this ongoing research. Essentially, the aim here is to characterise the form of the IRSL (>600nm) signal using various pre-treatments and measurement conditions in an attempt to understand the charge transfer kinetics of this relatively new luminescence signal. To allow us to observe the form of the far-red IRSL signal more effectively we have chosen to use the linearly modulated OSL technique (LM OSL), as introduced by Bulur (1996). The technique and the practical advantages of this system of measurement are described in the next section.

The linearly modulated OSL technique

Conventionally, optically stimulated luminescence, whether by visible or infrared wavelengths, has been carried out at constant excitation intensities (continuous wave or CW OSL). The subsequent radiative recombination is thus recorded as a monotonically decaying signal. During the alternative technique of LM OSL the stimulation light intensity is linearly increased from zero to a predetermined value during measurement, generating luminescence in the form of peaks. Consequently the LM technique allows greater visual clarity than using CW OSL, which can be useful for characterising the luminescence properties of minerals. If the form of the OSL is simple (i.e. a single 1st, 2nd order etc.) then, using derived analytical expressions (Bulur, 1996) a quick determination of the trap parameters can be achieved using the position and height of the OSL peak. For more complex, overlapping luminescence peaks (as is the case for quartz LM stimulated at 470nm (Bulur *et al.*, 2000), for example), where the parameters cannot be obtained so simply, curve fitting techniques can be used to approximate the LM OSL components more easily than with standard CW OSL.

In his first paper on the subject Bulur (1996) used an IR LED array to achieve ramped stimulation of natural feldspar grains. The linearly modulated (LM-) IRSL in the UV/blue emission band was recorded. A single peak was observed, whose shape he compared to curves of first, second and general kinetic order. While none could describe the whole LM curve, general order provided the best fit. In another paper (Bulur and Göksu, 1999), LM curves for K and Na feldspars were well approximated to the linear sum of three first order components.

Properties of the luminescence of feldspar

The mechanisms of production of feldspar luminescence are notoriously complex (see Duller, 1997, for review). Luminescence can be stimulated using visible wavelengths, and the efficiency was observed to increase with photon energy above 2eV (Poolton *et al.*, 1994). It is thought that these wavelengths induce charge transfer via the conduction band (Poolton *et al.*, 1994). Luminescence stimulated with low energy infrared photons at room temperature was attributed to an excitation resonance (Hütt *et al.*, 1988). One explanation for this was given by Poolton *et al.* (1994), which involved localised transitions via low-mobility band-tail states between donor-acceptor pairs.

Visocekas (1985) suggests recombination by wave-mechanical tunnelling is a likely mechanism of anomalous fading. Fading measurements made on laboratory timescales show the characteristic form of luminescence remaining after storage is proportional to log(storage time) (Spooner, 1993). Correlation was found between observed anomalous fading of TL and IRSL of feldspars and age underestimates (e.g. Wintle, 1973).

As stated previously, work by Zink and Visocekas (1997) showed that samples exhibiting anomalous fading in the blue/UV emission, did not fade noticeably in the far-red emission band. This emission was attributed to substitutional Fe^{3+} ions (Bos *et al.*, 1994). In studies of sanidines the emission was found to centre on 700-710nm (Dütsch and Krebetschek, 1997). The two emission bands (UV/blue and far-red) were found to behave similarly in terms of activation energies, dose response and bleaching of TL, but differently in terms of TL peak temperatures and kinetics (Zink and Visocekas, 1997).

With respect to the UV emission IRSL decay form, several authors, including Bailiff and Poolton (1991), have fitted IRSL decay curves to the form $1/(1+Bt)^2$, where B is a constant and t is illumination time, although this tends not to fit the initial portion of the decay successfully (Bailiff and Poolton, 1991). The reason for this has not been adequately explained. As stated in the previous section Bulur and Göksu (1999) fitted the LM IRSL from both K and Na feldspar samples to the sum of three first order components. The previous study to explore the form of the red emission using low energy infrared stimulation was performed by Fattahi and Stokes (2003b). They observed that IRSL (>600nm) decay curves were well approximated by three first order components also.

Here the form of the red IRSL emission of some feldspar samples, previously reported by Fattahi and Stokes (2003b) and Fattahi (2004), is examined using the linear

modulation technique. The dependence of form with various pre-treatment and measurement conditions is assessed. The LM IRSL (>600nm) was fitted to various analytical solutions and a discussion of the most appropriate approximation is undertaken.

2. EXPERIMENTAL DETAILS

Samples

The measurements were made on potassium feldspar extracted from either a selection of samples (WW1-4A, WW1-4B) collected from the United Arab Emirates, or a fluvioglacial sample from Ontario (Middle Wisconsinan deposits near St. Thomas, Ontario, Canada. Laboratory identification: Y7A). Details of sample information including their age, and preparation procedures are given in Fattahi (2001).

Measurement apparatus

A full description of the experimental apparatus is given in Fattahi and Stokes (2003c) and Fattahi *et al.* (2004) a summary of which is provided here. Experiments were carried out using a Risø TL DA-15 Automated TL/OSL system (Bøtter Jensen and Duller, 1992) fitted with a $^{90}Sr/^{90}Y$ beta source delivering ca 7 Gy·min^{-1}, and equipped with an infrared laser diode (λ_{peak} ca 830 nm), providing maximum stimulation intensity of 400 mW·cm^{-2}. Luminescence detection was performed using a D716A, bialkaline PMT that was equipped with an S 600 PHOTOCOOL thermoelectric refrigeration chamber, which allowed active cooling of the photocathode down to –20°C, to reduce thermal background. Filter combinations were used to allow transmission of either the red (590-650 nm; Fattahi and Stokes, 2003c), or UV (260-420nm; Bøtter Jensen and Duller, 1992) emissions respectively.

Measurement conditions

The linearity of the automated IR ramp was tested by directly measuring the light output from the IR laser. Neutral density filters were placed in front of the PMT to reduce the number of incident photons to a suitable level. The recorded excitation intensity was plotted against illumination time (see **Fig. 1**). Below ca 10% of maximum stimulation intensity the form of the ramp is non-linear. The reason for this is the absence of a feedback system for the laser in the reader model used (Bøtter Jensen *et al.*, 1999; this has since been corrected on further production models of the Risø reader). This produces a dramatically altered form of LM IRSL (see **Fig. 1** also), compared to similar feldspar LM IRSL curves recorded by Bulur and Göksu (1999). Clearly, it is not appropriate to fit the LM IRSL to analytical equations that are derived assuming a linear stimulation ramp.

A way to circumvent this problem is to measure the IRSL using constant stimulation intensity (CW IRSL). The IRSL decay curves can be transformed mathematically into the form that would be obtained using the linearly modulated technique. The transformation was first derived by Bulur (2000) and applied successfully to IRSL and green-stimulated OSL decays from K and Na feldspar samples. To convert a CW IRSL curve into an LM IRSL curve a new variable, u, is introduced, defined as follows:

$$u = \sqrt{2tT} \tag{2.1}$$

where t is time in seconds and T is the total LM measurement time (this can be any value, but $T = 2t_{CW}$, where t_{CW} is the total CW measurement time, has been chosen here to equate the total incident light energy of CW and LM IRSL). Then LM intensity is given by **Eq. 2.2**:

$$I_{LM} = \frac{I_{CW} u}{T} \tag{2.2}$$

By plotting I_{LM} vs u one obtains the same form as experimentally recorded LM IRSL curves. This transformation can be applied to convert first, second and general order kinetic IRSL decays, provided the mechanism of

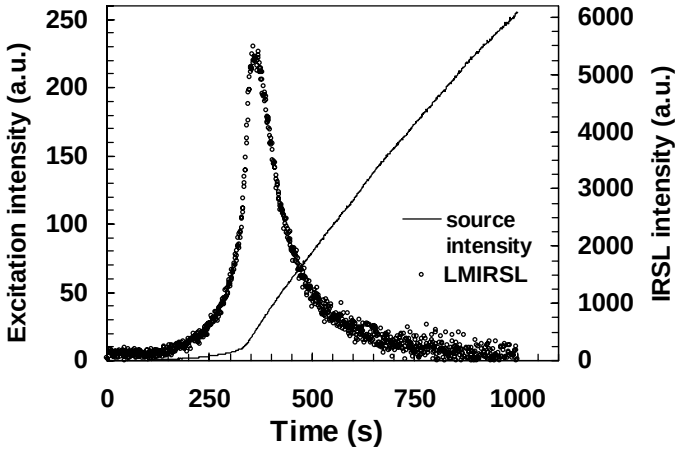

Fig. 1. *IR source intensity ramp, measured using neutral density filters placed in front of the PMT, and resulting LM IRSL.*

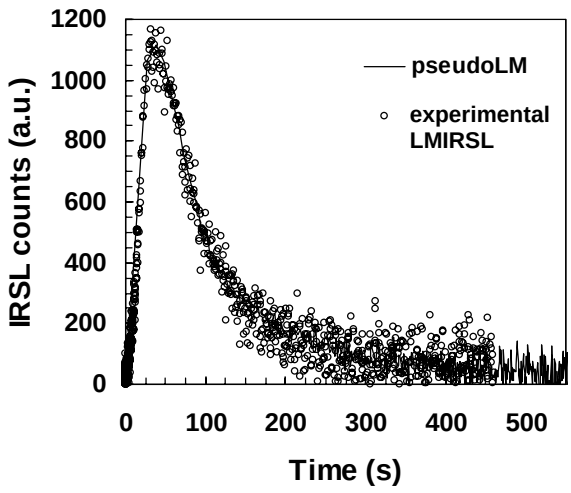

Fig. 2. *Comparison of mathematically transformed 'pseudo-LM IRSL' and experimental LM IRSL (plotted vs normalised source intensity – see section 2 for details).*

the detrapping of charge is independent of stimulation power. This method can take advantage of the greater signal stability of CW IRSL measurements and allows the transformed 'pseudo-LM IRSL' to be fitted to derived solutions describing LM IRSL. Measurements were preferentially made using this approach.

However, several initial experiments were performed using experimental linear modulation. In an effort to utilize these measurements it was found that plotting LM intensity vs excitation intensity produced a very similar form to the pseudo-LM curves. **Fig. 2** shows a comparison between transformed pseudo-LM IRSL and experimental LM IRSL (vs normalised stimulation power) for sample WW1-4A, which received 200Gy beta dose, and was preheated to 250°C in both cases. There is good agreement between the actual and pseudo-LM curves, implying that the transformation is a valid approximation for this sample. Therefore, in a few cases experimental LM measurements were included in the study. In the experiments described in section 3, when both experimental LM IRSL and pseudo-LM (transformed CW IRSL decays) were recorded the experiments produced equivalent results using the two approaches.

Deconvolution of LM IRSL curves

The resultant LM IRSL curves were deconvoluted using custom-written software incorporating a non-negative least squares algorithm (Lawson and Hanson, 1995) and/or a Levenberg-Marquardt algorithm in the mathematical software package, ORIGIN 4.1. The advantage of the first method is that no assumption is made concerning the number of constituent components.

The equations used in the deconvolution process were the same as those derived initially in Bulur (1996) for first, second and general order kinetic systems. For a single first order process, luminescence intensity, $L(t)$, is given by,

$$L(t) = n_0 \frac{bt}{T} exp\left(\frac{-bt^2}{2T}\right) \quad (2.3)$$

where, n_0 is proportional to the total number of trapped electrons, b is proportional to the photo-ionisation cross-section, and T is the total measurement time. Using the same nomenclature the equations for second and general order LM IRSL are as follows:

$$L(t,2nd) = \frac{n_0 \frac{bt}{T}}{\left(1+\frac{bt^2}{2T}\right)^2} \quad (2.4)$$

$$L(t,general) = n_0 \frac{bt}{T}\left[(\beta-1)\frac{bt^2}{2T}+1\right]^{\beta/(1-\beta)} \quad (2.5)$$

In the general order equation, β is a dimensionless positive real number ($\beta \neq 1$, $\beta \neq 0$).

3. EXPERIMENTAL RESULTS

Initial measurements of the LM IRSL emission

A single LM IRSL measurement was made on an aliquot of sample WW4A at 150°C following a laboratory beta irradiation of ~200Gy and preheat of 200°C for 30s. The LM IRSL (>600nm) is plotted against light source intensity (see section 2) in **Fig. 3** (far-red emission). A single peak is observed and a relatively long tail. The measurement was repeated to record the UV emission under the same conditions for comparison (also plotted in **Fig. 3**). While the UV emission set up produced a greater number of IRSL counts, the forms of the LM IRSL from the two spectral bands are almost identical.

Assuming that the emission wavelength band depends upon recombination centre type (as suggested by Zink and Viscoekas, 1997), the results imply that common trapped donor concentrations supply charge to the different recombination centres contributing to the red and UV emissions. It also implies that there is no effect on the rate of detrapping due to possible differences in the distance, or shared excited state, between the donor and different recombination centres, since the shape of the LM and position of the peak maximum are the same for the two emissions.

Influence of preheating on the form of LM IRSL (>600nm)

An experiment similar to pulse annealing was performed to look at the effect of preheating on the intensity and form of the LM IRSL (>600nm). A single aliquot was given a dose of 200Gy. The aliquot was subsequently preheated at 200°C for 30s before recording the LM IRSL (>600nm) at 150°C for 1000s from 0-0.9W·/cm^{-2}. The measurement procedure was repeated on the same aliquot for preheat temperatures between 200 and 400°C. Results for sample Y7A are shown in **Fig. 4** (a – LM IRSL

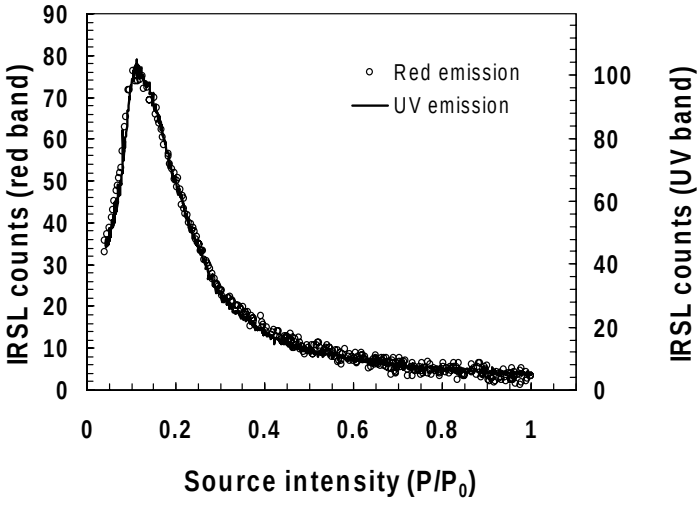

Fig. 3. *Comparison of red and UV LM-IRSL emissions. Both were measured at 150°C, following 200Gy beta dose, and 200°C preheat.*

(>600nm) curves, b – Peak height vs. preheat temperature). It was found that the total light sum from the 200°C measurements was relatively insensitive to previous heat/dose treatments, i.e. very little (<2%) sensitivity change was seen during the experiment. Therefore, we have displayed the raw IRSL (>600nm) data (after background subtraction), as no correction for sensitivity was required. Fattahi and Stokes (2003b) observed that, in general, the red emission of feldspar displays only very small changes in sensitivity with pre-treatment and measurement.

As can be seen in **Fig. 4a**, the total light sum recorded decreases with increasing preheat temperature. This is in agreement with observations of Fattahi and Stokes (2003b) using standard CW IRSL (>600nm) measurements. While the height of the LM IRSL (>600nm) curves decreases with increasing preheat temperature in **Fig. 4a**, the form of the curves remains similar. The position of the peak maximum is roughly constant, although the 200°C curve seems to display a small, superimposed peak not observed after higher preheats. This occurs just prior to the main peak position in all the other LM IRSL (>600nm) curves (the main peak maximum position is given by the dotted line in **Fig. 4a**). The form of the small, additional peak after the 200°C preheat may suggest the possibility that the remnant of a thermally unstable IRSL component is present and is thermally eroded by preheating to 225°C (further investigation concerning this feature will be presented elsewhere). However, it has relatively little impact on the form of the LM IRSL (>600nm). The overall position of the main peak maximum is otherwise unaffected by preheat temperature.

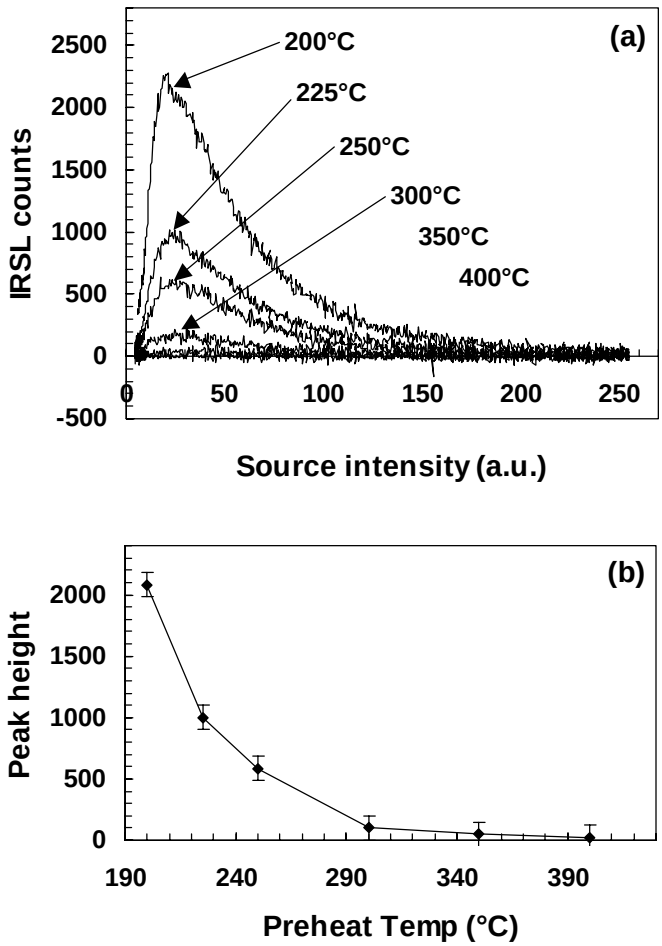

Fig. 4. *(**a**) LM IRSL (>600nm) curves following preheats between 200 and 400°C for sample Y7A. The LM curves were used to plot (**b**)*

That there is not a substantial influence of preheating on the form of the LM IRSL (>600nm) could indicate several possibilities. Firstly, there could be a single main component following first order kinetics, that is thermally eroded during high temperature preheats. However, the data could not be satisfactorily fitted to one first order component using curve-fitting, and further experiments also indicated that this could not be the case (see next sections). Thermal erosion of a single signal with a higher kinetic order can also be discounted, as this would result in a significant and systematic shift of peak position, due to change in charge concentration (the peak moving to longer times for lower signal levels). It is theoretically possible that there are several first order components with similar thermal stabilities, and erode in roughly equal proportions when exposed to high temperatures, so that there is negligible change in form with preheat temperature. A second possibility is that the radiative recombination centre is being eroded, hence there is little change in the form of the LM IRSL (>600nm) as the donor concentrations are negligibly affected by comparison. This was suggested by Trautmann *et al*. (2000) following measurements of the radioluminescence performed on feldspars at donor and acceptor emission wavelengths. They found that the IR radioluminescence (donor concentration) was not significantly affected by pulse annealing up to 450°C, whereas the blue and yellow radioluminescence (acceptor concentration) decreased at the same temperatures as for IRSL (UV/blue emission). They concluded that the loss of IRSL during preheating is due to the erosion of recombination centres. The same is likely to be the case for the IRSL (>600nm) emission. This possibility is further discussed in section 4.

In **Fig. 4b** the peak maximum is plotted vs preheat temperature. The same trend is seen if integrated IRSL is plotted. The experiment shows that there is negligible luminescence after preheating at 400°C. For a comparison between the two emission bands the above experiment was repeated for sample WW4A in both emission bands. The results are shown in **Fig. 5**. In **Fig. 5a** are the LM IRSL curves (UV emission). As observed in the red emission there is little effect of preheating temperature on the form of the LM IRSL (a fast, thermally unstable component after 200°C preheat is observed for both emissions that is not present after higher preheats). Peak height vs preheating temperature is plotted in **Fig. 5b** for both emissions. The red emission shows a similar form as sample Y7A (**Fig. 4b**), the UV emission appears to be more thermally stable at temperatures 200-300°C. However, both emissions are reduced to negligible levels by preheating to ca 400°C. Similar observations were obtained by Duller (1994) in a pulse annealing experiment for the IRSL (UV/blue emission) where natural and artificially

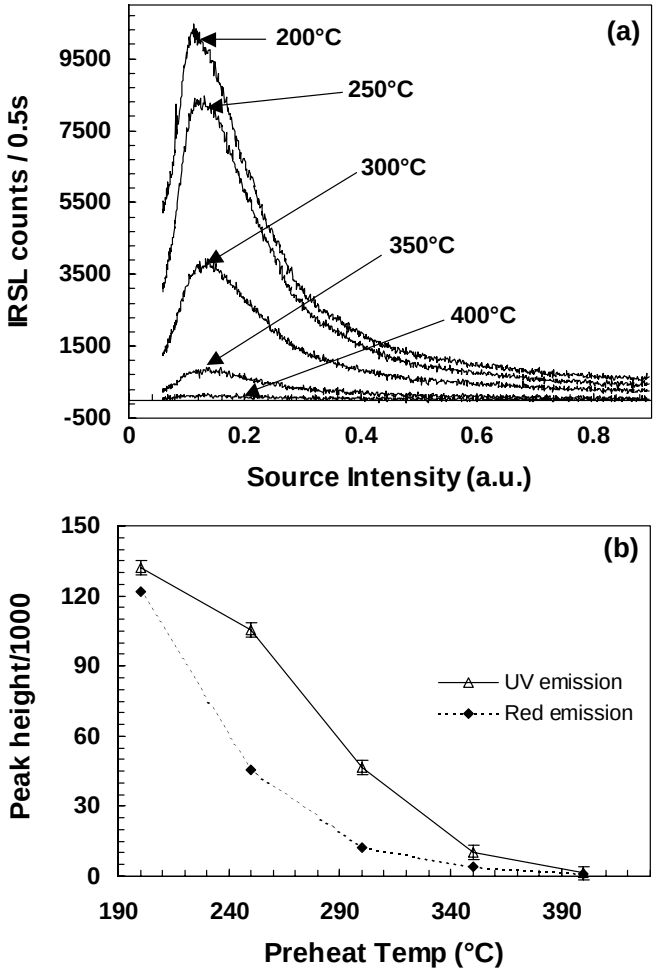

Fig. 5. *(**a**) LM IRSL curves (UV emission) following preheating between 200 and 400°C for sample WW1-4A. (**b**) Open symbols – peak height (of LM curves in (a)) for UV emission. Filled symbols – peak height for red emission of sample WW1-4a*

irradiated samples were completely thermally eroded by 400°C also and showed a similar form to the UV emission results presented here.

Effect of prior partial IR bleaching

To further elucidate the nature of the LM IRSL (>600nm) signal an experiment was performed to investigate the effect of prior partial IR bleaching on the IRSL (>600nm) form. The behaviour of the IRSL (>600nm) in response to partial bleaching should enable us to distinguish between some of the possible systems of kinetics of luminescence production.

For this experiment a single aliquot of WW4A was irradiated with 200Gy beta irradiation and preheated to 250°C for 30s. The aliquot was next bleached for n seconds using continuous wave IR stimulation at 150°C before reading out the pseudo-LM (see section 2) signal, also at 150°C (where n = 0 to 120s, at 280 mW·/cm^{-2}). Pseudo-LM IRSL (>600nm) measurements made without first partial bleaching were repeated several times throughout the experiment to monitor sensitivity change and this was observed to be negligible, as found previously.

The pseudo-LM (>600nm) curves following IR partial bleaching are plotted in **Fig. 6a**. The luminescence is completely depleted by 120s exposure to IR at 150°C (as observed by Fattahi and Stokes, 2003b, using CW IRSL). The shift of peak position with increasing prior partial bleaching is clearly seen. **Fig. 6b** (inset) shows a plot of the position of peak maximum, t_{max}, vs length of partial bleaching. That there is a shift to longer times with increasing partial bleaching indicates that the luminescence does not originate from one simple first order source (in which case the peak maximum would be constant). Other possibilities will be discussed in section 4.

Dose response

The dose response of the two feldspar samples were measured using a single aliquot regenerative dose method based on Murray and Wintle (2000). Previously aliquots were exposed to beta irradiations of 238Gy. Following dosing the aliquots were preheated at 250°C for 30s before recording the pseudo-LM IRSL (>600nm) (see section 2 for details). After each pseudo-LM IRSL (>600nm)

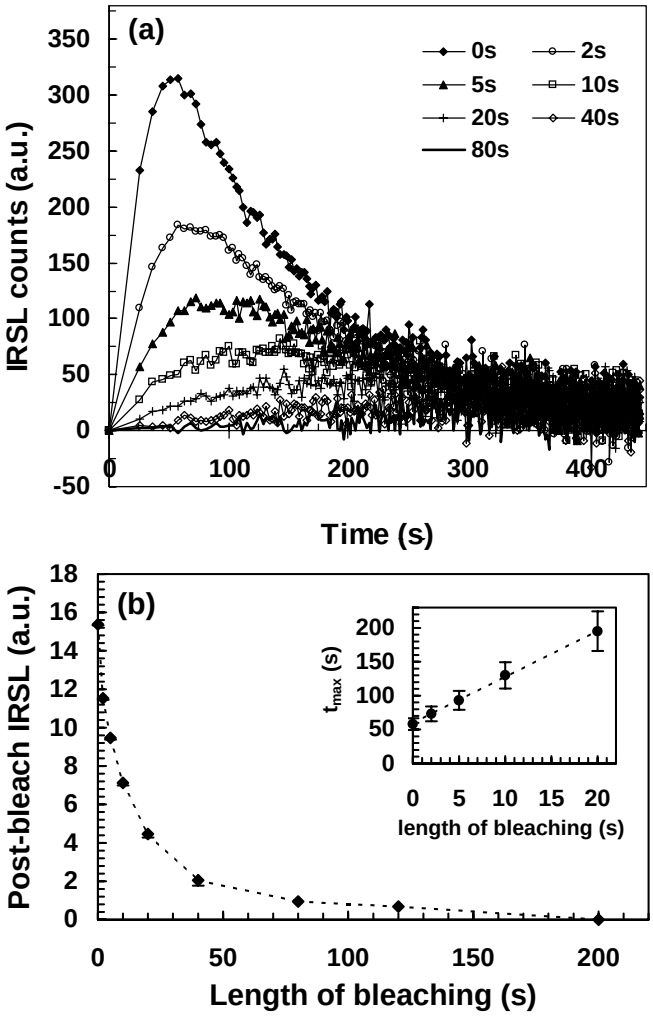

Fig. 6. *(**a**) Pseudo-LM IRSL (>600nm) curves following various lengths of IR bleaching at 150°C. (**b**) main figure shows pseudo-LM total integral (following prior bleaching). The inset shows the peak position, t_{max},*

measurement the IRSL (>600nm) from a smaller standard dose (ca 100Gy) was read out to monitor sensitivity change. The procedure was repeated for several different regenerative doses between 238Gy and 11900Gy. The standard dose IRSL (>600nm) total integral did not change significantly (<2%) throughout the experiment.

The pseudo-LM IRSL (>600nm) curves from sample WW1-4A for various doses are plotted in **Fig. 7**. The pseudo-LM IRSL curves resulting from the 7616Gy and 11900Gy are equivalent (overlap completely), indicating that dose saturation occurs at 7616Gy. This is reiterated more clearly in **Fig. 8a**, where the dose response curve, using the total light sum, is plotted (**Fig. 8b** shows the corresponding dose response curve for sample Y7A). Observations of the peak positions show that for doses below saturation, i.e. ≤ 3808Gy, there is no dependence on dose. Bulur and Göksu (1999) also found that LM OSL peak position was independent of dose, for the smaller range of doses they administered, using the UV emission of K and Na feldspar samples. They fitted their LM curves to the sum of three first order components, and noted that the constant peak position might imply that approximating the LM OSL to the linear sum of first order components may be valid.

A further observation is that at doses close to saturation (3808 – 11900Gy) the tails of the pseudo-LM IRSL (>600nm) curves all overlay, whereas the IRSL peaks increase up to 7616Gy. What this small change in form means is unclear at this stage. It may possibly imply that there is more than one first order component, one of

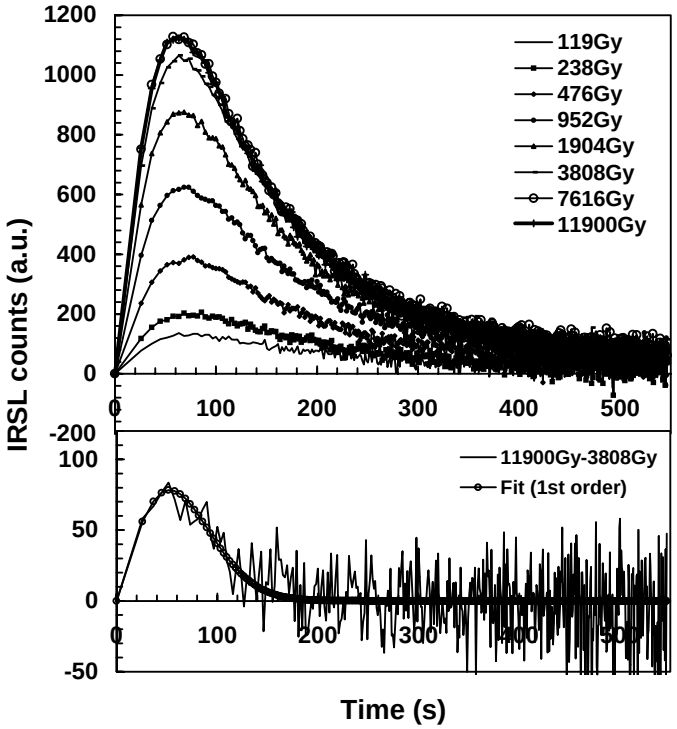

Fig. 7. *Upper figure shows pseudo-LM IRSL (>600nm) curves for sample WW1-4A after various administered β-doses (238-11900Gy). In the lower figure the data points for the 11900Gy LM IRSL (>600nm) minus the data for 3808Gy have been plotted. The subtraction curve has been fitted to a single first order LM component (see section 4 for details).*

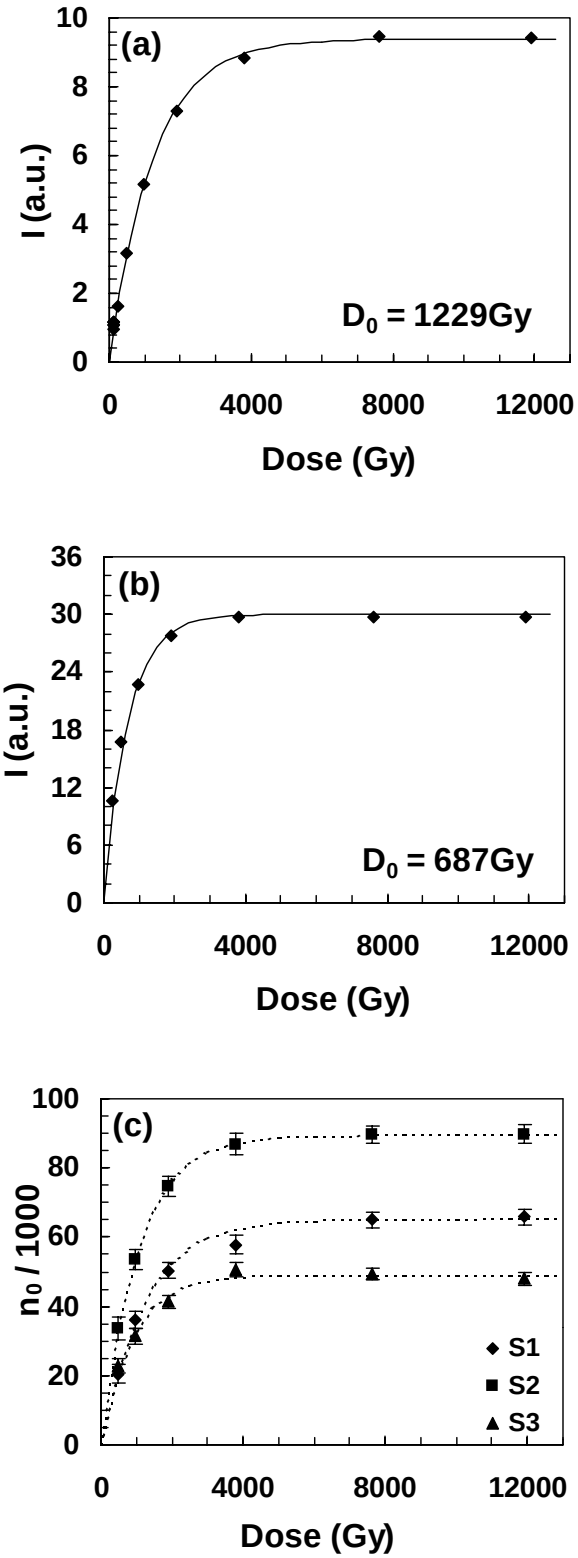

Fig. 8. *(**a**) Dose response curve for sample WW1-4A constructed using the total light sum from pseudo-LM IRSL (>600nm) measurements following various doses. (**b**) Dose response curve for sample Y7A, again using the total light sum. (**c**) The pseudo-LM IRSL (>600nm) curves for sample WW1-4A were fitted to three first order components, S1, S2 and S3. Component-resolved dose response curves were then plotted (using n_0, effective initial trapped charge concentration, vs β-dose.*

which saturates at slightly higher doses than the other(s). The possibilities are discussed in the next section. If the subtracted data points are plotted (i.e. data for 11900Gy minus data for 3808Gy) as in **Fig. 7b**, the pseudo-LM (>600nm) curve obtained can be fit to a single first order equation. However, the form of the resulting data is obscured by a large amount of noise. Although not plotted here, the other sample, Y7A, also showed the same pattern of behaviour at doses close to saturation, possibly also suggesting a single first-order component continuing to grow beyond the saturation level of the other components (further discussion below).

The dose response curves for both samples are plotted in **Fig. 8**, using the integral (0 to 450s) of the pseudo-LM IRSL (>600nm) from each given dose. The dose responses were successfully fitted to single saturating exponential functions. The parameter D_0, the characteristic dose where the slope of the dose response equals 1/e of the initial slope, was obtained for each sample. This was found to be 1229±116Gy for sample WW4A, and 687±47Gy for sample Y7A.

4. DISCUSSION AND INTERPRETATIONS

Shape of LM IRSL (>600nm)

The LM IRSL (>600nm) (measured at 150°C) of the feldspars investigated produced a single peak followed by a relatively long tail. The single peak suggested that the LM IRSL (>600nm) was perhaps composed of one component, however, attempts to fit the LM curves to derived equations for single first, second or general order kinetics (as given in section 2) were unsatisfactory. As Bulur and Göksu (1999) found for the UV emission of feldspar, the LM IRSL (>600nm) was best approximated with the sum of three first order components. An example fit to an LM IRSL (>600nm) curve is shown in **Fig. 9**, where the three deconvoluted components have been labelled S1, S2 and S3 (the curve was measured after preheating to 250°C, so that any thermally unstable components, such as observed after preheating to 200°C in **Fig. 4a**, were not present). Throughout the study the 'b' parameter (which

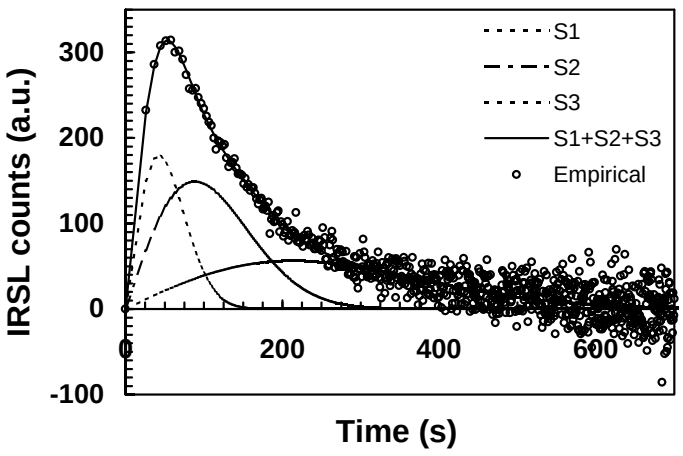

Fig. 9. *A typical LM IRSL (>600nm) curve measured at 150°C. The LM curve has been fitted to the sum of three first order components, S1, S2 and S3.*

is proportional to the photo-ionisation cross-section; see section 2 for details) of each of the components obtained through curve fitting has remained relatively consistent; b(S1) = 0.49-0.55, b(S2) = 0.1-0.13, b(S3) = 0.017-0.021.

The purpose of the experiments described here, and the main thrust of the discussion is to distinguish whether these components are in fact physically distinct, or merely an artefact of the deconvolution process.

Partial bleaching evidence

Following increasing prior IR partial bleaching periods the detrapping of the remaining IRSL became increasingly slow, as recognized by the movement of t_{max}, the peak position. This corroborates the finding, evidenced through the fitting process, that the mechanism of charge transfer is not a single first order process. If it were a single first order component no movement of t_{max} with prior partial bleaching would be observed. It was found that all the pseudo-LM (>600nm) curves measured during this experiment fitted well to three first order components, with near-constant decay constant parameters obtained between curves. Having fitted all the pseudo-LM (>600nm) curves, component-resolved plots of n_0 (proportional to the remaining trapped charge concentration) vs bleaching length were fitted to exponential functions that gave decay constants within errors of those found from the deconvolution of pseudo-LM (>600nm). The internal consistency achieved may indicate that the idea that the components have a physical basis is appropriate.

Poolton *et al.* (1994 and 2002) propose that when feldspars are exposed to IR stimulation recombination takes place between closely spaced donor-acceptor pairs via band-tail states. They suggest that, when illuminated, the nearest pairs recombine first. Then once stopped, the distribution of spacing between the remaining d-a pairs is significantly modified (no longer random), and the probability of recombination upon further IR illumination decreases, due to the increased average distance between pairs. This is as found from the partial bleaching experiment, and although we have chosen to fit our data to three components, this does not negate this possibility, as the two are not necessarily mutually exclusive, since the three components could relate (purely speculatively) to e.g. three different excited states required to allow recombination with centres at different distances, in other words a quantized effect.

Thermal stability evidence

Previous work (Zink and Visocekas, 1997) showed that the UV and far-red emissions possibly originate from different radiative recombination centres. If we assume that this is the case then the observation that the LM IRSL UV and red emissions overlap (**Fig. 3**) can be interpreted as common donor traps supplying charge to different recombination centres. This finding is possibly reiterated in **Figs 4**, **5a** and **b**, which compare the response to preheating of the red and UV/blue LM IRSL emissions. The form of the LM IRSL is unaffected by preheating temperatures (between 225°C and 400°C) in both emission bands. However, the total light sum produced

decreases following higher preheats. It is asserted that since the LM IRSL does not fit to a single first order solution, and there is no change in shape of the LM with preheating temperature, that the loss of signal is more likely to arise from the thermal erosion of recombination centres than other possible explanations (see section 3). This agrees with findings by Trautmann *et al.* (2000), who used radioluminescence at various wavelengths to directly observe the traps/centres filling. The shapes of the plots of peak height vs preheat (**Fig. 5b**) also seem to suggest that the UV centre is slightly more thermally stable than the red centre. Zink and Visocekas (1997) attributed differences in apparent thermal stability of red and UV TL emissions to thermal quenching and suggested that once corrected for the two centres had similar thermal stabilities. However, this cannot be the case here as all LM were made at constant temperature.

Furthermore, whether the thermal erosion is of traps or centres, for IRSL components of second or higher order the change in charge concentration (of either) would be expected to result in modification of the LM shape. That there is no major, systematic change in peak position with preheat temperature may suggest that first order mechanisms for charge transfer are most likely, adding more weight to the idea of multiple first order components contributing to the LM IRSL (>600nm). Note also that the results do not necessarily imply that the component traps have similar thermal stabilities, only that they are all apparently significantly more thermally stable than the red and UV centres.

Dose response evidence

The pseudo-LM IRSL (>600nm) resulting from the exposure of aliquots to various beta doses produced curves whose peak position was independent of dose (not close to saturation levels). This may imply that the assumption of first order kinetics for curve fitting is valid. It was found that close to saturation the initial portion of the pseudo-LM IRSL appeared to continue growing while the tail portion did not. Using the data from sample WW4A, subtraction of the data from two different relevant dosed pseudo-LM curves (**Fig. 7**, lower) produced a curve that could be fitted to a single first order peak (see previous section for details). The data are noisy, but note that the decay constant for the subtracted data is equivalent (within errors) to the fastest component when the raw data is fitted to three first order components, which supports the fitting of these three components to the pseudo-LM IRSL (>600nm). Curve fitting was used to obtain dose response curves for each of the three components obtained (S1, S2 and S3 – S1 being the fastest decaying of the components). **Fig. 8c** shows the initial charge concentration parameter n_0, obtained from fitting, vs laboratory dose. The dose response curves could be fitted to single saturating exponential functions, allowing estimation of D_0 for each component. The values obtained were $D_0(S1) = 1229 \pm 116$ Gy, $D_0(S2) = 1044 \pm 17$ Gy, $D_0(S3) = 902 \pm 97$ Gy. It appeared that the saturation level of the fastest component was a marginally higher than the two slower components.

5. CONCLUSIONS

Using the linearly modulated technique the infrared-stimulated red emission luminescence signal of feldspars has been studied. The form of the LM IRSL (>600nm) was found to be similar to the UV/blue emission, suggesting the possibility that the same donor concentrations contribute to both the red and UV IRSL emissions. The thermal stability of the far-red emission was found to be different to the UV/blue emission, supporting the suggestion of Zink and Visocekas (1997) that the emissions most likely originate from different radiative recombination centres, and further, that these radiative centres have different thermal stabilities.

All LM IRSL (>600nm) curves were best fitted to the sum of three first order components. The response of each component to a range of preheating, partial bleaching and irradiation pre-treatment provides evidence that these are indeed physically distinct components, rather than artefacts of the fitting procedure.

The D_0 of the first component of the IRSL signal (>600nm) of sample WW4A was found to be 1229 ± 116 Gy. This far exceeds typical D_0 values for quartz, while being less than the D_0 value (6.3 kGy) from RTL of volcanic quartz (Fattahi and Stokes, 2000b). It is not possible to draw firm conclusion regarding the extension of the dateable age range from this one sample, but such high dose saturation is consistent with previous findings where similarly large saturation values were obtained (e.g. Fattahi and Stokes, 2005).

The red IRSL signal of feldspar has been detected now in a wide range of samples and is found consistently to be more stable than the UV-blue luminescence emission. The presence of multiple signal components, with differing thermal/optical stabilities and considerable saturation doses, provides great potential for the accurate dating of Quaternary sediments over extended timescales.

ACKNOWLEDGEMENTS

MF and JSS are financially supported by Tehran University and NERC (ref: GT04/98/ES/231), respectively. We wish to thank an anonymous referee for critical review of the manuscript.

REFERENCES

Bailiff I.K. and Poolton N.R.G., 1991: Studies of charge transfer mechanisms in feldspars. *Nucl Tracks Radiation Meas* 18: 111-118.

Bos A.J.J., Piters T.M. and Ypma P.J., 1994: Thermoluminescence emission spectra and optical bleaching of oligoclase. *Radiation Measurements* 23: 349-353.

Bøtter Jensen L. and Duller G.A.T., 1992: A new system for measuring optically stimulated luminescence from quartz samples. *Nuclear Tracks and Radiation Measurements* 20: 549-533.

Bøtter Jensen L., Mejdahl V. and Murray A.S., 1999: New light on OSL. *Quaternary Science Reviews* 18: 303-309.

Bulur E., 1996: An alternative technique for optically stimulated luminescence (OSL) experiment. *Radiation Measurements* 26: 701-709.

Bulur E. and Göksu H.Y., 1999: IR-stimulated luminescence from feldspars with linearly increasing excitation light intensity. *Radiation Measurements* 30: 505-512.

Bulur E., Bøtter Jensen L. and Murray, A.S., 2000: Optically stimulated luminescence from quartz measured using the linear modulation technique. *Radiation Measurements* 32: 407-411.

Duller G.A.T., 1994: A new method for the analysis of infrared stimulated luminescence data from potassium feldspars. *Radiation Measurements* 23: 281-285.

Duller G.A.T., 1997: Behavioural studies of stimulated luminescence from feldspars. *Radiation Measurements* 27: 663-694.

Dütsch C. and Krbetschek M.R., 1997: New methods for a better internal ^{40}K dose rate determination. *Radiation Measurements* 27: 377-381.

Fattahi M. and Stokes S., 2000a: Red thermoluminescence (RTL) in volcanic quartz: development of a high sensitive detection system and some preliminary findings. *Ancient TL* 18: 35-44.

Fattahi M. and Stokes S., 2000b: Extending the time range of luminescence dating using red TL (RTL) from volcanic quartz. *Radiation Measurements* 32(5-6): 479-485.

Fattahi M., 2001: *Studies on red thermoluminescence and infrared stimulated red luminescence*. Unpublished D.Phil. thesis, University of Oxford.

Fattahi M. and Stokes S., 2003a: Dating volcanic and related sediments by luminescence methods: a review. *Earth Science Reviews* 62: 229-264.

Fattahi M. and Stokes S., 2003b: Red luminescence from potassium feldspar for dating applications: a study of some properties relevant for dating. *Radiation Measurements* 37: 647-660.

Fattahi M. and Stokes S., 2003c: Photomultiplier and filter combinations for the detection of relatively long wavelength (λ>600 nm) luminescence emissions from feldspar. *Ancient TL* 21: 25-34.

Fattahi M., 2004: The dependence of orange-red IRSL decay curves of potassium feldspar on sample temperature. Radiation Measurements 38(3): 287-298

Fattahi M. and Stokes S., 2004: Absorbed dose evaluation in feldspar using a single aliquot regenerative-dose (SAR) Infra red stimulated red luminescence protocol. *Radiation Measurements* 38: 127 – 134.

Fattahi M. Stokes S. and Lamothe M., 2004: Red luminescence emission from potassium feldspars stimulated by infrared. Ancient TL 22: 35-44.

Fattahi M. and Stokes S., 2005: Dating unheated quartz using a single-aliquot regenerative-dose red thermoluminescence protocol. *Journal of luminescence* 115: 19-31.

Hütt G., Jaek I. and Tchonka J., 1988: Optical dating: K-feldspars optical response stimulation spectra. *Quaternay Science Reviews* 7: 381-385.

Lamothe M. and Auclair M., 2000: The fadia method:a new approach in luminescence dating using the analysis of single feldspar grains. *Radiation Measurements* 32: 433-438.

Lawson C.L. and Hanson R.J., 1995: Solving least squares problems. *Classics in applied mathematics series, SIAM.*

Mejdahl V., 1985: Thermoluminescence dating based on feldspars. *Nuclear tracks and Radiation Measurements* 10: 133-136.

Murray A.S. and Wintle, A. G., 2000: Luminescence dating using an improved single-aliquot regenerative-dose protocol. *Radiation Measurements* 32: 57-73.

Poolton N.R.J., Bøtter-Jensen L., Ypma P.J.M. and Johnsen O., 1994: Influence of crystal structure on the optically stimulated luminescence properties of feldspars. *Radiation Measurements* 23: 551-554.

Poolton N.R.J., Ozanyan K.B., Wallinga J., Murray A.S. and Bøtter-Jensen L., 2002: Electrons in feldspar II: a consideration of the influence of conduction band-tail states on luminescence processes. *Physics and Chemistry of Minerals* 29: 217-225.

Spooner N.R.J., 1993: The validity of optical dating based on feldspar. Unpublished D.Phil. thesis, University of Oxford.

Spooner N.A. and Questiaux, D.G., 1989: Optical dating-Achenheim beyond the Eemian using green and infrared stimulation. *Synopses from a workshop on Long and Short Range Limits in Luminescence Dating.* Research Laboratory and the History of Art, Oxford University, occassoinal publication no. 9: 97-103.

Trautmann T., Krbetschek, M.R, Dietrich A. and Stolz W., 2000: The basic principle of radioluminescence dating and a localised transition model. *Radiation Measurements* 32: 487-492.

Visocekas R., 1985: Tunnelling radiative recombination in labradorite; its association with anomalous fading of thermoluminescence. *Nuclear Tracks and Radiation Measurements* 14: 149-154.

Visocekas R., 2000: Monitoring anomalous fading of TL of feldspars by using far-red emission as a gauge. *Radiation Measurements* 32: 499-504.

Wintle A.G., 1973: Anomalous fading of thermoluminescence in mineral samples. *Nature* 245: 143-144.

Zink A., 1996: Thermoluminescence des feldspaths. Emission par effet tunnel et par thermoluminescence dans l'infrarouge. Incidence sur la datation des felspaths. Thèse de Doctorat, Université de Bordeaux III, France.

Zink A. and Visocekas R., 1997: Datability of sanidine feldspars using the near-infrared TL emission. *Radiation Measurements* 27: 251-261.